The Different $[Fe_4S_4]^{3+}$ and $[Fe_4S_4]^{+}$ Species Created by γ Irradiation in Single Crystals of the $(Et_4N)_2[Fe_4S_4(SBenz)_4]$ Model Compound: Their EPR Description and Their Biological Significance

Jocelyne Gloux,† Pierre Gloux,‡ Bernard Lamotte,* Jean-Marie Mouesca,§ and Gérard Rius†

Contribution from the C.E.A./Département de Recherche Fondamentale sur la Matière Condensée SESAM/SCPM 85X, Grenoble, 38041, France

Received June 28, 1993®

Abstract: Extensive EPR studies of single crystals of the $[(C_2H_5)_4N]_2[Fe_4S_4(SCH_2C_6H_5)_4]$ compound and of its partially and fully deuterated counterparts show that many different $[Fe_4S_4]^{n+}$ ($n = 1$ or 3) paramagnetic species with $S = 1/2$ are created in these crystals after irradiation by γ rays. Five different $[Fe_4S_4]^{3+}$ species are identified: they correspond to the oxidized state of the high-potential iron–sulfur proteins. Moreover, two different $[Fe_4S_4]^{+}$ species are also identified which correspond to the reduced state of the ferredoxins. All these species have been characterized by their **g**-tensors. They have principal values in good agreement with the values corresponding to these states in the proteins. Concerning their principal directions, one feature has been found common to all the centers observed: the principal direction $\vec{V}_1$ associated with their greatest principal value g_1 is near the direction of the common perpendicular to the directions of the mixed-valence pair of iron atoms and of the ferric or the ferrous pair. The comparisons of these $\vec{V}_1$ directions made between the different centers have permitted us to give an explanation of their number and their diversity which are due to the different possibilities that the mixed-valence pair $Fe^{2.5+}$-$Fe^{2.5+}$ has to be localized on two particular atoms of the four iron atoms of the cubane cluster. The results obtained on the $[Fe_4S_4]^{3+}$ state suggest a new interpretation of the composite EPR spectrum of the oxidized high-potential *Chromatium vinosum* protein. Since the diverse components of this spectrum follow rather closely in *g*-values and saturation behaviors those of the $[Fe_4S_4]^{3+}$ states observed in the irradiated crystals, it is likely that these diverse components must also be due to different localizations of the mixed-valence pair on the irons of the active site.

I. Introduction

A new approach of the study of the paramagnetic states of the iron–sulfur cubanes introduced in previous publications from our laboratory[1-5] gives the possibility of carrying out very detailed studies by EPR and ENDOR of these entities constituting the active sites of many important iron–sulfur proteins. This method is based on the use of single crystals of synthetic model compounds, irradiated at high dose by γ rays. Its strength lies in the possibility of obtaining complete **g**-tensors and complete hyperfine tensors, allowing us to characterize in detail these species. This approach contrasts with the usual studies of the polynuclear iron–sulfur clusters in the proteins or in the model compounds which are all studied in the disordered state (i.e. frozen solutions or powders) and which, generally, cannot give access to these complete tensors.[6]

As it is well-known, the Fe_4S_4 cubanes can take three different mixed-valence redox states. Low-potential ferredoxins and a number of other iron–sulfur proteins have oxidized and reduced states which respectively correspond to the $[Fe_4S_4]^{2+}$ and $[Fe_4S_4]^{+}$ states, while the so-called high-potential proteins have oxidized and reduced states which correspond to the $[Fe_4S_4]^{3+}$ and $[Fe_4S_4]^{2+}$ states.[7] With regard to magnetic properties, the $[Fe_4S_4]^{2+}$ ground state is diamagnetic, while the two $[Fe_4S_4]^{+}$ and $[Fe_4S_4]^{3+}$ states are paramagnetic and relevant to EPR and ENDOR studies.[7]

The method that we develop is based on the use of single crystals of model compounds synthesized in the $[Fe_4S_4]^{2+}$ state. They are then irradiated with ionizing radiation (γ rays) in order to create simultaneously, in situ, the "oxidized" species $[Fe_4S_4]^{3+}$ and the "reduced" species $[Fe_4S_4]^{+}$, which both remain trapped in the crystalline matrix. The first species correspond to a trapped hole and the second ones to a trapped electron. They are present at low concentration and are oriented in crystals composed of the diamagnetic $[Fe_4S_4]^{2+}$ cubanes. These conditions are the best possible in order to perform high-resolution studies aiming to measure the **g** and hyperfine tensors associated with these different isolated states.

We have first demonstrated the feasibility of this method by EPR in single crystals of the $(Bu_4N)_2[Fe_4S_4(SC_6H_5)_4]$ synthetic model compound.[1,2] More recent developments have been made by EPR[4] and also by ENDOR on an $[Fe_4S_4]^{3+}$ state[3,5] in the model compound $(Et_4N)_2[Fe_4S_4(SBenz)_4]$. This last compound is more interesting than the previous one since its CH_2 groups are good analogs of the CH_2 groups of the cysteins in the proteins.

The purpose of the present article is to present the identification

† Also at the Université Joseph Fourier, Grenoble.
‡ Also with CNRS, Grenoble.
§ Present address: Department of Molecular Biology MB 1, Scripps Clinic and Research Foundation, 10666 North Torrey Pines, La Jolla, CA 92037.
® Abstract published in *Advance ACS Abstracts*, February 1, 1994.

(1) Gloux, J.; Gloux, P.; Lamotte, B.; Rius, G. *Phys. Rev. Lett.* **1985**, *54*, 599.
(2) Gloux, J.; Gloux, P.; Hendriks, H.; Rius, G. *J. Am. Chem. Soc.* **1987**, *109*, 3220.
(3) Rius, G.; Lamotte, B. *J. Am. Chem. Soc.* **1989**, *111*, 2464.
(4) Gloux, J.; Gloux, P. Communication at the Second European Inorganic Chemistry Seminar, Wiesbaden, Germany, April 16–20, 1990.
(5) Mouesca, J.-M.; Rius, G.; Lamotte, B. *J. Am. Chem. Soc.* **1993**, *115*, 4714.
(6) A general rule is that only the principal values of the tensors can be obtained in disordered samples. However, rudimentary information on the principal directions of the hyperfine tensors relative to those of the **g**-tensor may be obtained when the anisotropy of the effective **g**-tensors is large (see, for instance: Gurbiel, R. J.; Bolin, J. T.; Ronco, A. E.; Mortenson, L.; Hoffman, B. M. *J. Magn. Reson.* **1991**, *91*, 227). But one must be aware that this approach is only able, in the best cases, to give imprecise results which, moreover, are not free in ambiguities.
(7) (a) Lovenberg, W. *Iron-Sulfur Proteins*; Academic Press: New York, 1973; Vols. I and II; 1977; Vol. III. (b) Spiro, T. G. *Iron-Sulfur Proteins*; Wiley-Interscience: New York, 1982. (c) Matsubara, H.; Katsube, Y.; Wada, K. *Iron-Sulfur Protein Research*: Springer: Berlin, 1987. (d) Beinert, H. *FASEB J.* **1990**, *4*, 2483.

0002-7863/94/1516-1953$04.50/0

and extensive description by EPR of the different $[Fe_4S_4]^{3+}$ and $[Fe_4S_4]^{+}$ paramagnetic species ($S = 1/2$) appearing after γ irradiation of single crystals of the $(Et_4N)_2[Fe_4S_4(SBenz)_4]$ compound, in relation to concomitant ENDOR studies made on some of them. These studies have been pursued, in fact, in three different types of single crystals: (1) those obtained from the fully protonated compound, $[(C_2H_5)_4N]_2[Fe_4S_4(SCH_2C_6H_5)_4]$ (**1**); (2) those obtained from the partially deuterated compound, $[(C_2D_5)_4N]_2[Fe_4S_4(SCH_2C_6D_5)_4]$ (**2**); (3) those obtained from the fully deuterated compound, $[(C_2D_5)_4N]_2[Fe_4S_4(SCD_2C_6D_5)_4]$ (**3**).

The single crystals of compound **2** have been prepared especially in view of the ENDOR studies of the protons of the CH_2 groups;[5,8] but they have been also used for this study, their EPR lines being generally less broad than those found for the fully protonated crystals of **1**. Those made with the fully deuterated compound **3** have been especially prepared for this EPR study since they provide even sharper lines than the crystals of **2** and lead to a gain of resolution of about 3 in the EPR spectra with respect to those made with compound **1**. Moreover, in the present study we have used much higher integrated doses of γ irradiation than in the previous one,[1,2] resulting in the possibility of identifying more paramagnetic species.

This study presents two main interests on which we will focus. We will see that we observe several varieties of $[Fe_4S_4]^{3+}$ and $[Fe_4S_4]^{+}$ species. Thus, a major purpose of this work will be to interpret this diversity by giving an explanation which establishes a relationship between the different **g**-tensors and the essential features of the geometric and electronic structures of the species considered. Moreover, since ENDOR studies are currently pursued in our laboratory on several of these paramagnetic species,[3,5,8,9] the results of these studies will be related to the present ones. The second important point will be to examine the biological significance of these results, i.e. the relation appearing between the species identified in this study and those found in the proteins. This will give us the possibility of proposing for the $[Fe_4S_4]^{3+}$ state a new and more satisfying interpretation of the EPR spectra of the oxidized state of the *Chromatium vinosum* high-potential protein than those proposed before.[10]

II. Experimental Section

1. Preparation of $(Et_4N)_2[Fe_4S_4(SBenz)_4]$ and Its Partially and Fully Deuterated Counterparts. Single crystals of the three different compounds **1**–**3** have been used for this study. All these compounds have been prepared from very pure $FeCl_2 \cdot 4H_2O$ made from 99.999% pure iron. Compound **1** has been obtained by the classical method of Christou and Garner.[11] The preparation of the selectively deuterated compound **2** and $(C_2D_5)_4$-NI has been already described in ref 5. We will only summarize here the other syntheses.

(a) Preparation of $C_6D_5CD_2SH$. This compound has been prepared in five successive steps. Deuterated benzoic acid has been obtained from perdeuterated bromobenzene, magnesium, and CO_2 in a Grignard reaction. Then, methyl benzoate has been made from thionyl chloride and methyl alcohol. It was then reduced by $LiAlD_4$ to give fully deuterated benzyl alcohol, which was then attacked by thionyl chloride to give fully deuterated benzyl chloride. The compound $C_6D_5CD_2SMgBr$ has then been prepared from magnesium, sulfur, and the fully deuterated benzyl chloride; it has been decomposed in acidified water, giving rise to the deuterated toluene thiol, extracted by distillation. Some disulfide being also formed, it has been reduced separately by $LiAlH_4$ in order to complete the quantity of $C_6D_5CD_2SH$ obtained. The global yield from bromobenzene has been 14%; the toluene thiol has been found deuterated to about 98% by NMR.

(b) Preparation of $[(C_2D_5)_4N]_2[Fe_4S_4(SCD_2C_6D_5)_4]$ (3). The $[(C_2H_5)_4N]_2[Fe_4S_4(S$-*t*-$Bu)_4]$ compound has been prepared by the method of Christou and Garner.[11] The final compound has been obtained by ligand exchange with toluene thiol, while for the preparation of the deuterated complex, $[(C_2D_5)_4N]_2[Fe_4S_4(S$-*t*-$Bu)_4]$ is first prepared from deuterated tetraethylammonium iodide and finally obtained by ligand exchange with the deuterated toluene thiol. The different steps of these preparations have been conducted in a glovebox under argon atmosphere (1 ppm of O_2).

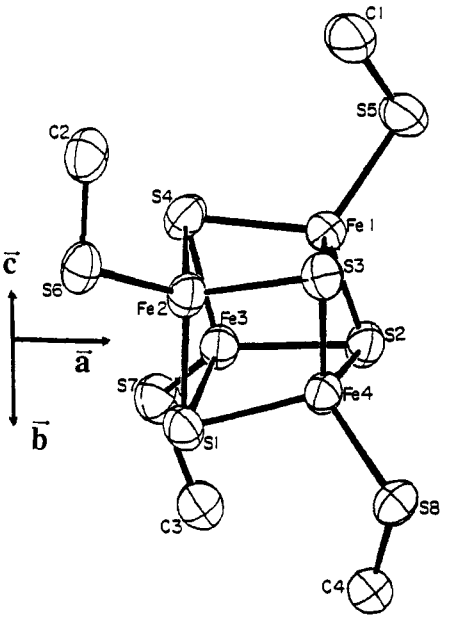

Figure 1. Representation, taken from the X-ray study,[12] of the central part of the $Fe_4S_4(SCH_2C_6H_5)_4$ core, with its orientation given with respect to the $\vec{a}$, $\vec{b}$, $\vec{c}$ directions of the unit cell. These unit vectors, $\vec{a}$, $\vec{b}$, $\vec{c}$, are represented by their projections in the sheet plane.

2. Preparation of the Crystal Samples, Structural Information, and EPR Methodology. Single crystals weighing several milligrams have been obtained by a transport method, the compound dissolved in acetonitrile being placed in tight tubes under argon atmosphere in a temperature gradient. These crystals were then irradiated under argon atmosphere by γ rays in a ^{60}Co source at room temperature, at doses between 0.2 and 1 MGy. The crystallographic structure of the compound studied has been published by Averill et al.[12] It crystallizes in the monoclinic space group $P2_1/c$ ($\beta = 95.8°$) with $Z = 4$. The single crystals generally grow with a well-developed face corresponding to the *ac* plane, with its greatest dimension along the *a* axis. X-ray experiments using the Laüe method have been made in order to determine $\vec{a}$, $\vec{b}$, $\vec{c}$ directions of the unit cell on the natural faces of the crystals. An orthogonal reference frame *abc** with $\vec{c}^* = \vec{a} \otimes \vec{b}$ has been defined from this morphology. In order to facilitate the discussions of the following paragraphs, we have represented in Figure 1 the central part of the $Fe_4S_4(SCH_2C_6H_5)_4$ core oriented with respect to the $\vec{a}$, $\vec{b}$, $\vec{c}$ directions of the unit cell. It must be remarked that the crystallographic structure presents the peculiarity that the directions perpendicular to the cubane faces, i.e. the $\overrightarrow{Fe_xFe_y} \otimes \overrightarrow{Fe_zFe_t}$ directions (with $x, y, z, t = 1, 2, 3$, or 4), are near the *a*, *b*, *c** directions.

The EPR spectra have been obtained either on a Varian E-109 EPR spectrometer or on a Bruker ER 200 D-SRC spectrometer, both equipped with an Oxford Instruments ESR-9 continuous flow helium cryostat. They have been recorded in three perpendicular planes *ab*, *bc**, and *c***a*. Each paramagnetic center has two inequivalent sites for a general orientation of the static magnetic field. When the magnetic field vector is either contained in the mirror glide plane *c***a* or aligned along the *b* screw axis, these two sites become equivalent in the EPR spectra.

III. Experimental Results

Prior to γ irradiation, the crystals used for this study have been found nearly always free from paramagnetic impurities, within the limits of EPR sensitivity. When they are irradiated by γ rays, their EPR spectra show the presence of numerous lines associated with diverse paramagnetic centers. All these lines are spread over about 500 G around $g = 2$, and they exhibit relatively large anisotropies as a function of orientation. An important remark, already made about the $(Bu_4N)_2[Fe_4S_4(SC_6H_5)_4]$ crys-

(8) Rius, G.; Mouesca, J.-M.; Lamotte, B. To be published.
(9) Giori, C.; Rius, G.; Lamotte, B. To be published.
(10) (a) Antanaïtis, B. C.; Moss, T. H. *Biochim. Biophys. Acta* **1975**, *405*, 262. (b) Dunham, W. R.; Hagen, W. R.; Fee, J. A.; Sands, R. H.; Dunbar, J. B.; Humblet, C. *Biochim. Biophys. Acta* **1991**, *1079*, 253.
(11) Christou, G.; Garner, C. D. *J. Chem. Soc. Dalton Trans.* **1979**, 1093.
(12) Averill, B. A.; Herskowitz, T.; Holm, R. H.; Ibers, J. A. *J. Am. Chem. Soc.* **1973**, *95*, 3523.

tals,[1,2] is that *none of these signals can be assigned to free radicals* created on the aromatic phenyl rings of the ligands or on the aliphatic counterions or SCH_2 groups of the ligands. In effect, these radicals would have been recognizable by resolved proton hyperfine structures which do not appear here and also by nearly isotropic g-tensors very different from those reported in the following.

These different EPR lines have a large range of intensities, and they exhibit different saturation behaviors. They also differ largely by the range of temperatures inside which they can be observed. This is why we have made the determination of their angular variations at different temperatures (typically 4, 10, 30, and 70 K), with different values of the microwave power. This method has allowed us to determine the g-tensors of the greatest possible number of them, in spite of quite severe problems of overlap between all the lines. That permits us in effect to select a smaller number of lines dominating in intensity the spectra for a given temperature and a given value of the microwave power and thus to measure conveniently their angular variations. Finally, seven different species have been identified by this method. But additional small EPR lines belonging to other paramagnetic centers have also been observed at high gain in these irradiated crystals.

The line widths in the EPR spectra at 4 K of the protonated crystals made with compound **1** vary from about 6 to 12 G depending on the crystal orientation and on the centers considered. These line widths are essentially due to the unresolved hyperfine interactions with the protons. Consequently, the complete deuteration of the compound must lead to a gain of resolution of about 3, the magnetogyric ratio of the deuterium being 6.5 times smaller than that of the proton and its nuclear spin being 1 instead of 1/2. This is indeed the case since the EPR line widths of the deuterated crystals of compound **3** vary between about 2 and 4 G. The line widths given by the crystals of compound **2** are intermediate between those obtained with the two types of crystals discussed above. In practice, the deuterated crystals made with compounds **2** and **3** have been mostly used to unravel important details insufficiently resolved in the protonated crystals. They generally contain the same kinds of paramagnetic species as in the protonated crystals. However, some particular differences appear in the fully deuterated crystals, which will be specified in section IV-5.

The EPR spectrum of Figure 2a of an irradiated single crystal of the protonated $[(C_2H_5)_4N]_2[Fe_4S_4(SCH_2C_6H_5)_4]$ compound **1** taken along the *b* axis exhibits five lines corresponding to seven different paramagnetic centers that we have labeled I, II, III, IV, V, I_R, and II_R (the EPR lines of the centers I, II, and V are superposed for this orientation). The angular variations of the different centers in the three perpendicular planes *ab*, *bc**, and *c*a* are shown in Figure 3. The continuous curves correspond to theoretical fits based on a Hamiltonian containing the Zeeman interaction $\tilde{H}\cdot\tilde{g}\cdot\tilde{S}$ involving a spin $S = 1/2$. The g-tensors associated with the seven different species labeled above are calculated from these fits and are given in Table 1. The ambiguities appearing in the determination of the relative signs of the off-diagonal terms of the g-tensors before diagonalization have been solved by using the knowledge of the $\tilde{a}$, $\tilde{b}$, $\tilde{c}$ directions determined on the crystals studied and, in addition, by tracing the angular variations of the EPR lines in a fourth plane.

IV. Analyses of the Results

The g-tensors presented in Table 1 must be classed in two categories. The first one involves the paramagnetic centers I, II, III, IV, and V with average *g*-values greater than 2. Following all the literature and also our previous analyses,[1-4] these centers are identified with the $[Fe_4S_4]^{3+}$ state, which can be viewed as "trapped holes", i.e. cubanes having lost one electron by ionization. They correspond therefore to the oxidized state of the high-potential iron–sulfur proteins active site. In effect, their principal

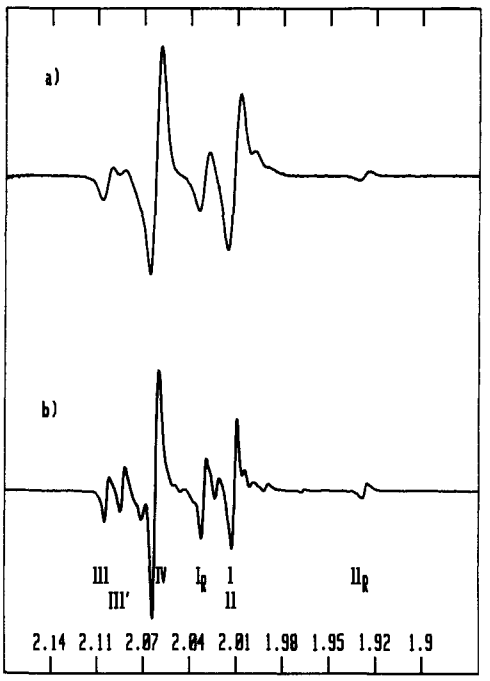

Figure 2. EPR spectra at 15 K of γ-irradiated single crystals of $(Et_4N)_2[Fe_4S_4(SBenz)_4]$, with the static magnetic field along the *b* axis of the crystals. We have indicated the EPR lines of the $[Fe_4S_4]^{3+}$ centers I, II, III, and IV and also those of the two centers I_R and II_R of the $[Fe_4S_4]^{+}$ type (note that, for this direction, the EPR lines of the centers I, II, and V are superposed): (a) spectrum of the crystal made with the $[(C_2H_5)_4N]_2[Fe_4S_4(SCH_2C_6H_5)_4]$ compound; (b) spectrum of the crystal made with the fully deuterated compound $[(C_2D_5)_4N]_2[Fe_4S_4(SCD_2C_6D_5)_4]$. Note the presence of the center III', which, in this case, has the same intensity as the center III.

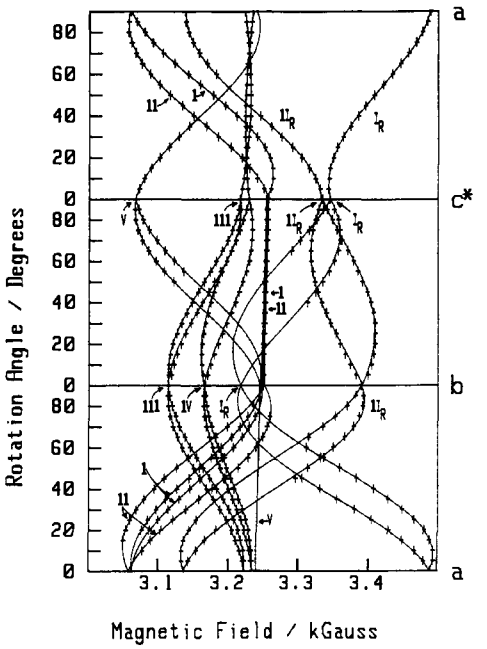

Figure 3. Angular dependencies in the three orthogonal planes *ab*, *bc**, and *c*a* of the EPR lines corresponding to the five centers I, II, III, IV, and V of the $[Fe_4S_4]^{3+}$ type and to the two centers I_R and II_R of the $[Fe_4S_4]^{+}$ type. The crosses (+) correspond to experimental points, and the continuous curves represent computer fits.

g-values g_1, g_2, and g_3 (always defined in the following such that $g_1 > g_2 > g_3$) are in good agreement with the values already found for these proteins. The comparison with the protein *g*-values will be discussed in more detail in section V-1. The second category of species involves the paramagnetic centers I_R and II_R, which have average *g*-values lower than 2. They can be viewed as "trapped electrons", i.e. cubanes of the crystal having captured

Table 1. Principal Values and Principal Directions of the g-Tensors of the Seven Paramagnetic Centers Identified in the Irradiated Crystals, i.e. the Five Different $[Fe_4S_4]^{3+}$ Species Respectively Labeled I, II, III, IV, and V and the Two $[Fe_4S_4]^{+}$ Species Labeled I_R and II_R[a]

paramagnetic center	isotropic g-value (g_{av})	principal g-values	principal direction cosines with respect to a	b	c*
I	2.053	g_1 = 2.142	+0.979	−0.048	−0.201
		g_2 = 2.013	+0.020	+0.990	−0.140
		g_3 = 2.004	+0.205	+0.133	+0.970
II	2.053	g_1 = 2.146	+0.974	−0.204	+0.095
		g_2 = 2.009	+0.048	+0.600	+0.798
		g_3 = 2.003	+0.220	+0.774	−0.595
III	2.054	g_1 = 2.101	−0.059	+0.996	−0.071
		g_2 = 2.039	−0.629	+0.018	+0.777
		g_3 = 2.023	+0.775	+0.090	+0.625
IV[b]	2.038	g_1 = 2.070	−0.089	+0.962	−0.259
		g_2 = 2.026	+0.680	+0.248	+0.690
		g_3 = 2.018	+0.727	−0.115	−0.676
V	2.055	g_1 = 2.135	−0.137	+0.087	+0.987
		g_2 = 2.017	+0.862	+0.501	+0.075
		g_3 = 2.014	−0.488	+0.861	−0.144
I_R	1.954	g_1 = 2.043	−0.142	+0.947	−0.288
		g_2 = 1.948	+0.048	+0.297	+0.954
		g_3 = 1.871	+0.989	+0.121	−0.088
II_R	1.992	g_1 = 2.087	+0.990	−0.133	+0.039
		g_2 = 1.971	−0.090	−0.401	+0.911
		g_3 = 1.917	+0.105	+0.906	+0.409

[a] The principal values have been called g_1, g_2, and g_3 with $g_1 > g_2 > g_3$, and their corresponding principal directions have been labeled $\vec{V}_1$, $\vec{V}_2$, and $\vec{V}_3$. [b] The g-tensor reported here for the center IV is slightly different from the one reported in refs 3 and 5.

and stabilized one electron, and must be identified with the $[Fe_4S_4]^{+}$ state. The centers I_R and II_R correspond to the reduced state of the active site of the ferredoxin proteins (as indicated by the R index).

The spectrum of Figure 2a gives an idea of the relative concentrations of the different paramagnetic centers that we find in the irradiated crystals. However, we must point out that they are strongly crystal dependent. Among the $[Fe_4S_4]^{3+}$ species, the center IV is the most intense, while the center I just follows in intensity. The centers II and III are, more often, between 2 and 5 times less abundant than the center IV, and there is a difference of roughly 2 orders of magnitude between the center V and the center IV. As for the "reduced" $[Fe_4S_4]^{+}$ species, we find that the intensity of the center I_R is, in mean value, of the same order as those of the "oxidized" species II or III, while II_R is about 4 times less intense than I_R. This means that, globally, the $[Fe_4S_4]^{+}$ centers are less numerous than the $[Fe_4S_4]^{3+}$ centers and that only a minor fraction of the electrons released by the γ irradiation are effectively permanently trapped under the form of the $[Fe_4S_4]^{+}$ species. All these centers are quite stable at room temperature since we do not observe important decreases of their EPR lines for single crystals kept under argon atmosphere several months after irradiation. We recall that, apart from the special case of the center V, we are only speaking here of the most intense EPR signals that we have always found in all the crystals grown from the high-purity compounds. However, it is clear that other small EPR lines are observed which correspond to other paramagnetic centers, in particular if sufficiently large crystals are irradiated at sufficiently high doses. But their EPR lines being completely masked for the major part of the orientations by the more intense lines pertaining to the centers described here, we have not attempted to determine their g-tensors in order to identify them.

IV-1. Analysis of the g-Tensors of the Five Centers of the $[Fe_4S_4]^{3+}$ Type. The g-tensors of the five $[Fe_4S_4]^{3+}$ centers are close to axiality. They are quite similar, in this respect, to those already attributed to the oxidized state of high-potential proteins.[10,13] But they appear, however, relatively dissimilar between them, and we can class them *in three different categories*.

Table 2. Values for the Different Paramagnetic Centers I, II, III, IV, V, I_R, and II_R of the Angle Θ Between the Principal Direction $\vec{V}_1$ Associated with the Greatest Principal Value of the EPR Site of Table 1 and the Corresponding Direction $\overrightarrow{Fe_xFe_y} \otimes \overrightarrow{Fe_zFe_t}$ Referred to the Crystallographic Site Having its Coordinates Given in Ref 12[a]

paramagnetic center	greatest principal g-value	Fe_xFe_y x =	y =	Fe_zFe_t z =	t =	Θ angle
I	g_1 = 2.142	1	4	2	3	10°
II	g_1 = 2.146	1	4	2	3	10°
III	g_1 = 2.101	1	2	3	4	11°
IV	g_1 = 2.070	1	2	3	4	16°
V	g_1 = 2.135	1	3	2	4	11°
I_R	g_1 = 2.043	1	2	3	4	20°
II_R	g_1 = 2.087	1	4	2	3	6°

[a] The index x, y, z, and t of the iron atoms given in the table are the ones allowing, for each center, a relevant comparison between these two kinds of directions, i.e. those leading to a relatively small value of Θ. The comparisons made with the second EPR site give similar angles except for the II and II_R centers, where Θ values about 10° greater are found. Thus, although it is not possible to identify the crystallographic site by EPR, it is nevertheless possible to establish the correlation existing between each $\vec{V}_1$ direction and a well-characterized direction normal to cubane faces.

The first category corresponds to the two centers I and II, which are very similar. They both have nearly axial g-tensors, alike g_{av} values, and relatively large anisotropies. They also have another feature in common: the principal axis (of quasi-axiality) $\vec{V}_1$—associated with the greatest principal value g_1—has nearly the same direction for the two centers, and it is near the direction of the *a* axis of the crystal.

The second category corresponds to the centers III and IV. Their g-tensors are less anisotropic than the previous ones and somewhat more rhombic. Their principal axis $\vec{V}_1$ of near-axiality is also nearly the same for the two centers, the two axes both being near the *b* axis of the crystal. However, it must be noticed that the center III has a g_{av} value distinct from the g_{av} value of the center IV, but the same as those of the centers I and II. By contrast, the anisotropy of its g-tensor is intermediate between the one of center IV and those of the centers I and II.

Finally, we have to consider the center V, which has also a nearly axial g-tensor, with the same anisotropy as found for the centers I and II. But it must be classified in a third category because its principal axis of quasi-axiality $\vec{V}_1$ is close to the c^* direction that we have defined from the crystal structure.

Thus, an obvious discrimination in three categories is achieved by linking the $\vec{V}_1$ tensor directions with the crystallographic directions *a*, *b*, c^*. This makes sense in connection with the peculiarity of the present crystallographic structure that the directions perpendicular to the cubane faces, i.e. the $\overrightarrow{Fe_xFe_y} \otimes \overrightarrow{Fe_zFe_t}$ directions, are close to the *a*, *b*, c^* directions. We present in Table 2 the values of the small angle Θ found for each of the centers between the principal direction $\vec{V}_1$ and the corresponding $\overrightarrow{Fe_xFe_y} \otimes \overrightarrow{Fe_zFe_t}$ cubane direction. It is useful to recall here the results of the previous study made on irradiated crystals of the $(Bu_4N)_2[Fe_4S_4(SC_6H_5)_4]$ synthetic model compound,[1,2] where two $[Fe_4S_4]^{3+}$ paramagnetic centers called B and B′ had been identified.[2] It had been also found in that case that the principal axes of near-axiality of these two centers associated with the greatest principal value g_1 were near directions normal to cubane faces.

IV-2. Explanation of the Multiplicity of Paramagnetic $[Fe_4S_4]^{3+}$ Centers Observed. First, we recall that the Mössbauer studies of the high-potential *Chromatium* protein[14]—as well as those made

(13) (a) Blum, H.; Salerno, J. C.; Cusanovich, M. A. *Biochem. Biophys. Res. Commun.* **1978**, *84*, 1125. (b) Beinert, H.; Thomson, A. J. *Arch. Biochem. Biophys.* **1983**, *222*, 333.

(14) (a) Dickson, D. P. E.; Johnson, C. E.; Cammack, R.; Evans, M. C. W.; Hall, D. O.; Rao, K. K. *Biochem. J.* **1974**, *139*, 105. (b) Middleton, P.; Dickson, D. P. E.; Johnson, C. E.; Rush, J. D. *Eur. J. Biochem.* **1980**, *104*, 289.

on the $[Fe_4S_4(S\text{-}2,4,6\text{-}(i\text{-}Pr)_3C_6H_2)_4]^-$ model compound[15]—have established that in the $[Fe_4S_4]^{3+}$ oxidation state there are two distinct pairs of iron atoms. The charge and the spin delocalization are not uniform, two equivalent α irons of a delocalized mixed-valence pair $Fe^{2.5+}$–$Fe^{2.5+}$ having to be distinguished from two equivalent β irons of a ferric pair Fe^{3+}–Fe^{3+}. In this simple description, the electronic structure of this state has therefore a C_2 axis of symmetry defined by the common perpendicular $\overrightarrow{Fe^{2.5+}Fe^{2.5+}} \otimes \overrightarrow{Fe^{3+}Fe^{3+}}$ to the $Fe^{2.5+}$–$Fe^{2.5+}$ and Fe^{3+}–Fe^{3+} directions. Following this consideration, and in agreement with the previous observations made on two $[Fe_4S_4]^{3+}$ centers B and B′ in the $(Bu_4N)_2[Fe_4S_4(SC_6H_5)_4]$ crystals,[2] the proximity of the principal direction of near-axiality $\vec{V}_1$ with a direction normal to the opposite cubane faces supports the existence of such an idealized C_2 axis for each of the centers.

The above results lead us to the interpretation that *the multiplicity of $[Fe_4S_4]^{3+}$ centers observed in these crystals is due to different possibilities which exist (amounting to a maximum of six) to localize the $Fe^{2.5+}$–$Fe^{2.5+}$ mixed-valence pair at the level of two particular iron atoms of the cubane.* For the centers I and II, this means more precisely that the mixed-valence pair is either localized on the Fe_1 and Fe_4 pair or on the Fe_2 and Fe_3 pair of iron atoms. These two centers being clearly distinct, one of them must correspond to one localization, while the other corresponds to the remaining one. We deduce in the same way for the centers III and IV that their mixed-valence pair must be localized either on the Fe_1 and Fe_2 pair or on the Fe_3 and Fe_4 pair and, at last, that it must be localized for the center V either on the Fe_1 and Fe_3 pair or on the Fe_2 and Fe_4 pair. We must remark that we are unable in each case to choose, with the EPR information alone, between the two possible localizations. Besides, the deviations of Θ from 0 reported in Table 2 come from the fact that the iron ions are not really equivalent in the two pairs, their local environments being inequivalent in the crystalline structure. The ^{57}Fe ENDOR study of the center IV bears testimony of this fact, since the hyperfine tensors measured are found inequivalent for the two irons in the mixed-valence pair as well as for those of the ferric pair.[3]

Let us consider now the principal directions $\vec{V}_2$ and $\vec{V}_3$ corresponding to the principal values g_2 and g_3. Beginning with the case of centers III and IV, which is the most clear, we find that $\vec{V}_2$ of center III is at 10° from $\vec{V}_3$ of center IV and also that $\vec{V}_3$ of center III is at 11° from $\vec{V}_2$ of center IV. Thus, we notice that the second and the third principal directions are approximately interchanged when we go from the center III to the center IV and conversely. This also suggests that one of these two centers must have its mixed-valence pair localized on the irons 1 and 2, while the other must have this pair localized on the irons 3 and 4. Moreover, these $\vec{V}_2$ and $\vec{V}_3$ principal directions of the centers III and IV are relatively close to the Fe_1Fe_2 and Fe_3Fe_4 directions of the cubane deduced from the X-ray structure determination.[12] In effect, for the center III, the direction $\vec{V}_2$ is at 8° from the Fe_3Fe_4 direction (associated with the site 1 of the cubane in the crystal; see the caption of Table 2) and the direction $\vec{V}_3$ is at 8° from the Fe_1Fe_2 direction. And for the center IV, the direction $\vec{V}_2$ is at 17° from the Fe_1Fe_2 direction, while the direction $\vec{V}_3$ is at 6° from the Fe_3Fe_4 direction.

As noticed before, it is not possible to go further in the attribution of particular centers to defined localizations of the mixed-valence pair with the consideration of the g-tensors alone. However, these attributions become possible with the help of ENDOR experiments which measure tensors of hyperfine interactions with nuclei having nonzero nuclear spins. This task has been first undertaken with an ^{57}Fe ENDOR study which has proved that the center IV has its mixed-valence pair localized on the irons 3 and 4.[3] A proton ENDOR study of this center IV has also been made more recently, and it has permitted us to deduce the electron spin populations on the different irons and to confirm definitively this conclusion.[5] Such studies are pursued on other centers in these crystals. A similar, but for the moment incomplete, ENDOR study of the center III seems to indicate that it has indeed its mixed-valence pair localized on the irons 1 and 2.[9]

We have to examine now, in the same way as above, the group constituted by the centers I and II. We do not find in this case such a correspondence between their respective $\vec{V}_2$ and $\vec{V}_3$ axes as the one found above for the centers III and IV. In effect, $\vec{V}_2$ of center I is at 31° from $\vec{V}_3$ of center II, and $\vec{V}_3$ of center I is at 30° from $\vec{V}_2$ of center II. The cause of these divergences is that the $\vec{V}_2$ and $\vec{V}_3$ directions of the center II are rather close to Fe–Fe directions, while those of the center I are not. For the center II, $\vec{V}_2$ is at 12° from the Fe_2Fe_3 direction, while $\vec{V}_3$ is at 17° from the Fe_1Fe_4 direction. By constrast, for the center I, $\vec{V}_2$ and $\vec{V}_3$ are respectively at 7° of $\overrightarrow{Fe_1Fe_2} \otimes \overrightarrow{Fe_3Fe_4}$ and at 9° of $\overrightarrow{Fe_1Fe_3} \otimes \overrightarrow{Fe_2Fe_4}$, i.e. much closer to these directions than to the Fe_1Fe_4 and Fe_2Fe_3 directions. These discrepancies are not negligible, but they are not very significant because these g-tensors are nearly axial. In effect, in such a situation, a minor perturbation is probably able to change rather drastically the directions of the principal axes perpendicular to the axis of quasi-axiality. We must add that the proton ENDOR study of the center I indicates that this center has its mixed-valence pair localized on the Fe_2 and Fe_3 atoms.[5] Unfortunately, we have no ENDOR data concerning the center II, but we feel it is reasonable to suppose that its mixed-valence pair is localized on the Fe_1 and Fe_4 atoms, in spite of the imperfect correspondence discussed above between the $\vec{V}_2$ and $\vec{V}_3$ directions of the centers I and II.

Following the identification of the four main centers, we have searched the two last ones for which the mixed-valence pair would be localized on the two remaining positions. First investigations among the low-intensity EPR lines of the spectra of fully protonated crystals of compound **1** showed from their angular dependencies two possible candidates. But these lines could only be observed for quite delimited portions of orientations where they were not masked by the much stronger lines belonging to the first four centers. Finally, with the use of the deuterated crystals **2** and **3**, it has been possible for one of the two remaining centers, namely the center V, to obtain portions of curves of angular variations in the two perpendicular planes bc^* and c^*a sufficient to deduce its g-tensor with little uncertainty.[16] But this has not been possible for the sixth one because only small portions of the curve that we may attribute to it are clearly visible in the spectra of the deuterated crystals **3** near the c^* axis in the bc^* and c^*a planes. These portions correspond to minima of the magnetic field along these directions and thus to a maximum g-value of ≈ 2.12, close to the c^* axis. This extremum value close to the c^* axis and relatively similar to the one found for the center V renders this attribution plausible. But since the lines corresponding to this center are masked for all the other orientations by those of the other centers, it has not been possible to further ascertain its identification.

IV-3. Analysis of the g-Tensors of the Two I_R and II_R Centers of the $[Fe_4S_4]^+$ Type. The g-tensors of the species I_R and II_R are relatively similar to each other, their main difference being at the level of their g_{av} values, which, anyway, are both smaller than 2. Their principal g-values are fairly distinct from those attributed to the $[Fe_4S_4]^{3+}$ centers; by contrast, they are in good agreement with the values corresponding to those of the reduced state $[Fe_4S_4]^+$ of the ferrodoxin proteins which are described by a $S = 1/2$ state. They are also characterized by relatively large g-anisotropies and by marked rhombicities. With respect to their principal directions, we see in Table 2 that the $\overrightarrow{Fe_1Fe_2} \otimes \overrightarrow{Fe_3Fe_4}$ and

(15) Papaefthymiou, V.; Millar, M. M.; Münck, E. *Inorg. Chem.* **1986**, *25*, 3010.

(16) No EPR lines attributed to the center V have been observed in the *ab* plane. We have supposed that they have an isotropic or quasi-isotropic angular dependence and that they are masked by the much more intense EPR lines of the other centers. The fits made in the bc^* and c*a planes effectively led to resonance fields equal for the *a* and the *b* directions.

$\overline{Fe_1Fe_4} \otimes \overline{Fe_2Fe_3}$ directions are close to the $\vec{V}_1$ principal directions of respectively I_R and II_R. An analogous situation has been already found for an $[Fe_4S_4]^+$ center called A in the $(Bu_4N)_2[Fe_4S_4(SC_6H_5)_4]$ crystals.[2] These diverse observations lead us to extrapolate to these $[Fe_4S_4]^+$ centers the type of model developed above for the $[Fe_4S_4]^{3+}$ centers. In effect, the previous Mössbauer studies on the $[Fe_4S_4]^+$ state have also permitted the distinction, in first approximation, of two different pairs of iron atoms, i.e. a delocalized mixed-valence pair $Fe^{2.5+}$–$Fe^{2.5+}$ and a ferrous pair Fe^{2+}–Fe^{2+}.[14] Then, as before for the $[Fe_4S_4]^{3+}$ state and with the same limitations, we can consider that the electronic structure of the $[Fe_4S_4]^+$ state has a C_2 axis of symmetry defined by the common perpendicular $\overline{Fe^{2.5+}Fe^{2.5+}} \otimes \overline{Fe^{2+}Fe^{2+}}$ to the $Fe^{2.5+}$–$Fe^{2.5+}$ and Fe^{2+}–Fe^{2+} directions. Thus, we propose that the center I_R has its mixed-valence pair localized either on the Fe_1 and Fe_2 atoms or on the Fe_3 and Fe_4 atoms and that, for the center II_R, the mixed-valence pair is localized either on the Fe_1 and Fe_4 atoms or on the Fe_2 and Fe_3 atoms. Preliminary results of a proton ENDOR study of the center I_R seem to indicate that, indeed, its mixed-valence pair is localized on the Fe_3 and Fe_4 atoms.[9]

Analyzing the principal directions $\vec{V}_2$ and $\vec{V}_3$ of the two centers, we do not find any unambiguous relation with defined directions of the cubane structure. It must be noted that an ambiguity also exists for the analogous center A in the $(Bu_4N)_2[Fe_4S_4(SC_6H_5)_4]$ crystals.[2] In the present study, in the case of the center II_R the $\vec{V}_2$ and $\vec{V}_3$ directions are close to Fe–Fe directions since $\vec{V}_2$ is at 16° from the Fe_1Fe_4 direction while $\vec{V}_3$ is at 17° from the Fe_2Fe_3 direction; but, by contrast, the principal directions of the center I_R are closer to the $\overline{Fe_1Fe_3} \otimes \overline{Fe_2Fe_4}$ and $\overline{Fe_1Fe_4} \otimes \overline{Fe_2Fe_3}$ directions than to the $\overline{Fe_1Fe_2}$ and $\overline{Fe_3Fe_4}$ directions. In this case, $\vec{V}_2$ is at 13° from the $\overline{Fe_1Fe_3} \otimes \overline{Fe_2Fe_4}$ direction, while $\vec{V}_3$ is at 15° from the $\overline{Fe_1Fe_4} \otimes \overline{Fe_2Fe_3}$ direction.

Finally, we have not identified more than two $[Fe_4S_4]^+$ centers. It is possible that some of the remaining $[Fe_4S_4]^+$ centers exist: they would then correspond to some of the low-intensity EPR lines that we see at $g < 2$ values in the c^*a plane and also near the a axis is the ab plane. But these weak signals not being visible elsewhere, we could not measure their g-tensors and identify them.

IV-4. Behavior of the $[Fe_4S_4]^{3+}$ and $[Fe_4S_4]^+$ Centers as a Function of Temperature and Saturation. The fact that the different $[Fe_4S_4]^{3+}$ and $[Fe_4S_4]^+$ centers exhibit fairly different behaviors as a function of temperature and microwave saturation has been already evoked at the beginning of section III. Let us describe this somewhat more precisely here for the most important centers: I, II, III, IV, and I_R.

We find that these different centers nearly saturate in the same way at 7 K. But when the temperature is raised above this temperature, the center IV begins to saturate much less than the others. Its power for half-saturation at 15 K is about 50 mW, while it is around 1 mW for the others. The difference is quite striking at 26 K because the plot of $S/\sqrt{P}$ over $\sqrt{P}$ is linear up to 200 mW for the center IV, while for the other centers (namely, I, II, III, and I_R), the power for half-saturation is found between 10 and 30 mW.

Moreover, the EPR lines of the center IV in the fully protonated crystals begin to broaden at 30 K, and the broadening is then very abrupt above; they are no longer detectable above 40 K. Those of the center III begin to broaden at 30 K, but much more gradually, and they disappear around 60 K. Those of the center I_R begin to broaden at 50 K and then abruptly above, and they disappear above 60 K. Finally, those of the centers I and II begin to broaden at 60 K and then gradually above; they disappear around 120 K.

These observations indicate that the center IV has a first excited state giving rise to rapid electronic relaxation that we have roughly evaluated to be 50–80 cm^{-1} above the ground state, following estimations based on the variations of their EPR line width with temperature. This energy difference for the center IV appears to be very significantly lower than those relative to the other centers, for which the situations are rather contrasted. The center III (companion of the center IV) must have its first excited state located clearly higher above the one estimated for the center IV. In the cases of the centers I and II, the energy difference would be even greater, i.e. 2–3 times bigger than for the center IV. These estimations are essentially qualitative elements useful in the comparisons between the different centers. But more serious information on the positions of the first excited state would be obtained from further measurements of the electronic relaxation times as a function of temperature.

IV-5. Peculiar Observations Made in the Completely Deuterated Crystals: Multiplicity of the Different Paramagnetic Centers Observed. The use of fully deuterated single crystals of compound **3** has given a gain of EPR spectral resolution of 3 and permitted us to identify the center V (and, maybe also, the sixth $[Fe_4S_4]^{3+}$ center), as we have seen before. But the spectra of these crystals have also revealed supplementary features which are *well-resolved satellite EPR lines* adjacent to the principal lines and are associated with the centers described above. Some of them can be seen in Figure 2b, in comparison with the same spectrum given by the protonated crystal in Figure 2a. Some of these satellite lines are, in fact, already visible as more or less distinguishable shoulders in Figure 2a; but, there are also rather important differences between the deuterated and protonated crystals which appear at the level of the relative intensities of the lines pertaining to the different centers and between the intensities of the satellites lines with respect to the main ones. This is striking, for instance, for the center III, where a variety of it that we call III′ has an EPR line of the same intensity as the one corresponding to the center III in the deuterated crystal (Figure 2b), while it is much less intense in the protonated crystal (Figure 2a). But these intensities are also crystal dependent, since inspection of several irradiated crystals of the completely deuterated compound **3** shows that, in fact, the EPR line of the variety III′ can be either greater or lower than the EPR line of the center III. The centers I and II are particularly rich in satellite lines since we can count up to five satellite lines for them, but which are resolved and thus well apparent only along the a axis direction of the crystal and around it.

The essential characteristic of these different satellite lines is that their angular variations follow in parallel to the main centers with which they are associated. They have also the same behavior as a function of temperature and of saturation as those of the main centers. Since these satellite lines are not of equal intensity and are no symmetrically disposed around the main ones, we have to discard the hypothesis that they would be due to nearby paramagnetic centers in electron–electron dipolar interaction. Consequently, they must correspond to paramagnetic centers having g-tensors very similar to those of their main species. That is to say that they have practically the same principal directions as those of the main species to which they are associated and that their principal values vary only by a few percent from those of their corresponding main species.

IV-6. Conjectures on the Simultaneous Trapping of the Different Species in the Irradiated Crystals. We can only make some speculations in order to explain the existence of the multiplicity of the different centers described above. Their occurrence must be discussed in the context of another important question: how is it possible, considering a given $[Fe_4S_4]^{3+}$ or $[Fe_4S_4]^+$ state in a given single crystal, that there is creation and stabilization of different centers having their mixed-valence pair localized on different pairs of irons? The hypothetical answer (already discussed before[3]) that we propose is that *they would be trapped in the vicinity of preexisting defects in the crystals.* Since we have prepared our crystals with very pure compounds (especially iron), we discard the possibility that the most important paramagnetic centers are associated with impurities. The ENDOR spectra, in particular, do not reveal the presence of such eventual impurities. We favor, by contrast, the possibility of

their association with structural defects such as stacking faults or dislocations. Then, the paramagnetic centers would be preferentially created and self-trapped at certain favorable sites in the vicinity of particular stacking faults or in the zones of strain field surrounding the dislocation lines. Such a trapping mechanism carries an explanation of their diversity and also permits us to explain why the relative intensities of the different centers differ from one irradiated crystal to another. The existence of the satellite lines observed in the deuterated crystals would be justified by the same kind of explanation; but, for a given center, they would correspond to quite minor geometrical differences expressed by nearly identical tensors.

The large differences in EPR line intensities found for the different centers indicate that the probabilities of trapping into these different configurations are, accordingly, fairly different. In the case of the $[Fe_4S_4]^{3+}$ centers, the fact that all the possibilities of localization of the mixed-valence pair are indeed realized seems to indicate that their total energies must be very close with respect to each others. We must precise, in addition, that we have not found (within the range of temperatures where the EPR lines are observable) the least indication of dynamical exchange such as jumps between two or more different localizations of the mixed-valence pair on the cubane cluster. These different centers are thus stable and trapped in a static and defined way in the crystal, and their concentration only slowly decreases (more or less depending on the centers) on the scale of months at room temperature.

V. Discussion: Biological Significance of the Results Obtained

We want now to examine the usefulness of the above results concerning the spectral interpretations of the iron–sulfur proteins and their related synthetic models. We will limit this discussion, in practice, to the other EPR and NMR measurements made on the $[Fe_4S_4]^{3+}$ state since, up to now, we have obtained in our single crystal studies much more complete results by EPR and ENDOR on this state than on the $[Fe_4S_4]^{+}$ state.

V-1. Connections with the EPR Spectra of the $[Fe_4S_4]^{3+}$ State in the High-Potential *C. vinosum* Protein. The EPR spectra of the oxidized state of *C. vinosum* are particularly unusual and interesting because then appear more complex than the classical powder or frozen solution spectra, exhibiting three singularities corresponding to the three principal values of a g-tensor ascribed to a single $S = 1/2$ paramagnetic species. They have been studied in detail by Antanaïtis and Moss,[10a] while the effects of freezing on these spectra of protein solutions containing high NaCl concentrations have been recently discussed by Dunham et al.[10b] Those of the same protein where the inorganic sulfur atoms are substituted by selenium atoms have been discussed by Moulis et al.[17]

Antanaïtis and Moss have concluded in their study that the EPR spectra of *C. vinosum* are due to the superposition of two principal signals[18] and a third, minor one. They attribute an axial tensor with $g_{\parallel}^1 = 2.120$ and $g_{\perp}^1 = 2.040$ to the first and most important signal and a less anisotropic and more rhombic tensor with $g_1^2 = 2.087$, $g_2^2 = 2.055$, and $g_3^2 = 2.040$ to the second significant signal.[19] An important difference between these two signals is that the axial signal is much more easily saturable than the rhombic one. Besides, Moulis et al. have distinguished in the Se-substituted protein four different signals to which they attribute the following sets of g-values:[17] $g_1 = 2.168$, $g_2 = 2.034$, and $g_3 = 2.028$; $g_1 = 2.152$, $g_2 = 2.038$, and $g_3 = 2.027$; $g_1 = 2.117$, $g_2 = 2.044$, and $g_3 = 2.035$; $g_1 = 2.085$, $g_2 = 2.048$, and $g_3 = 2.035$. The first corresponds to the major axial signal in the native protein.[20] It appears that there exists, in fact, a rather close similarity between the variety of signals observed in oxidized *C. vinosum* and those attributed to the $[Fe_4S_4]^{3+}$ centers in the irradiated crystals. In effect, if we focus our discussion in each case on the two main signals, it is found that the axial signal 1 of *C. vinosum* has g-values quite similar in axiality and anisotropy to those of the centers I and II, while its rhombic signal 2 is relatively similar in g-anisotropy and rhombicity to the centers III and IV. Moreover, the saturation behavior of the axial signal 1 of the HiPIP protein is similar to the one of the centers I and II, while the saturation behavior of the rhombic signal 2 of the protein is similar to the one of the center IV. Consequently, we are led to suppose that the two main signals distinguished in the spectrum of oxidized *C. vinosum* are very analogous to the centers I and IV in our crystals, respectively.

However, another hypothesis has been made in the recent article from Dunham et al.[10b] concerning the EPR signals observed in *C. vinosum* other than the dominant axial one. These EPR measurements have been recently duplicated by Gaillard[21] on the HiPIP of *C. vinosum* and also made on the recently isolated[22] *Chromatium tepidum* HiPIP, which shows a complex EPR spectrum in its oxidized state identical to the one of *C. vinosum*. The article of Dunham et al. is, for his part, dedicated to the influence of NaCl on the EPR spectra of oxidized *C. vinosum*. It suggests, from the analysis of these spectra, the possibility of freezing-induced dimerization in the salt solutions of the protein. But, in addition, these authors also propose an interpretation of the native protein spectrum which is different from the one of Antanaïtis and Moss. In effect, they associate the so-called "low-field ramp" at $g \approx 2.13$ with the bump that Antanaïtis and Moss had previously attributed to the g_1 of their second signal (g_1^2), so that they characterize for their part the second significant signal of the protein spectrum by the following g-tensor: $g_1^2 \approx 2.13$, $g_2^2 = 2.07$, and $g_3^2 = 2.04$.

We must point out our disagreement with this alternative interpretation. Careful observations made by Gaillard[21] show that the "low-field ramp" at $g \approx 2.13$ saturates easily (about in the same way as the peak at $g = 2.12$), while the bump at $g = 2.085$ saturates much less. Consequently, there is a difference in saturation behavior occurring between the two features of the EPR spectrum that Dunham et al. consider as associated with a unique signal. This difference is, in fact, already clearly visible in Figure 4a of the article of Antanaïtis and Moss, showing the K-band spectra of the protein at 20 K for different values of the microwave power attenuation. Moreover, careful examination of this figure and of the spectra taken at X-band[21] shows in addition that a relatively broad feature around $g \approx 2.10$ also exists (it has already been noted at $g = 2.108$ in ref 17). In effect, the inspection of Figure 4b of ref 10a shows that this feature, which must constitute an element of a weak signal, is indeed present at this place since the simulated spectrum made without taking it into account is tangential to the base line at this place. Moreover, this feature becomes more and more visible in Figure 4a of ref 10a when the microwave power is increased because it saturates less easily than the peak adjacent to it at $g = 2.12$.

In summary, this discussion of the EPR spectra of oxidized *C. vinosum* led us finally to the following conclusions:

(i) We virtually agree with the g-values that Antanaïtis and Moss have attributed to the two principal signals 1 and 2, i.e. $g_{\parallel}^1 = 2.120$ and $g_{\perp}^1 = 2.040$ for the first one, and $g_1^2 = 2.087$, $g_2^2 = 2.055$, and $g_3^2 = 2.040$ for the second one.[19]

(ii) We suggest that two additional signals distinct from the previous ones and less visible than them, which will be noted 3

(17) Moulis, J.-M.; Lutz, M.; Gaillard, J.; Noodleman, L. *Biochem.* **1988**, *27*, 8712.

(18) Following the terminology used in the articles cited in ref 10, we use the two terms "signal" or "component" in order to characterize a particular paramagnetic species defined by the three principal values of its g-tensor.

(19) Antanaïtis and Moss have attributed an equal weight to these two main species, but this point seems doubtful. Other authors (see in particular ref 17) consider that the component with the axial tensor is always the major one, the proportion of the rhombic one varying somewhat from sample to sample.

(20) It must be noted that the presence of selenium increases the g-anisotropy of the different signals observed.

(21) Gaillard, J. Private communication.

(22) Moulis, J.-M.; Scherrer, N.; Gagnon, J.; Forest, E.; Petillot, Y.; Garcia, D. *Arch. Biochem. Biophys.* **1993**, *305*, 186.

and 4, are also present with lower intensities in the EPR spectra of these proteins. Their visible parts would correspond respectively to the "low-field ramp" at $g \approx 2.13$ and to the broad signal at $g \approx 2.10$. The g-tensors associated with the $[Fe_4S_4]^{3+}$ state being generally close to axiality, we may crudely suppose that these two supplementary signals that we label 3 and 4 probably correspond respectively to $g_\parallel^3 \approx 2.13$, $g_\perp^3 \approx 2.03$–2.04 and to $g_\parallel^4 \approx 2.10$, $g_\perp^4 \approx 2.03$–2.04.[23] We find it interesting to point out their approximate likeness with the two centers of intermediate intensity found in our crystals: the signal 3 is in effect relatively analogous to the center II, while the signal 4 is relatively comparable to the center III.

(iii) Consequently, four different signals (or species) must be distinguished in the spectra of the oxidized *C. vinosum* and *C. tepidum* proteins, the same number having been found previously in the Se-substituted *C. vinosum*.[17] Their g-tensors, and also the behaviors as a function of temperature and saturation of their corresponding EPR lines, present a real similarity with those of the four $[Fe_4S_4]^{3+}$ centers I, II, III, and IV of large or intermediate intensity that we have identified in our irradiated crystals. This is why we are led to propose an explanation of their origin and of their diversity which is similar to the one that we have proposed for our irradiated crystals. We thus suggest that the composite spectra shown by the *C. vinosum* and *tepidum* proteins are associated with four different localizations of the mixed-valence pair on the four iron atoms of their iron–sulfur cubane active site. They can be seen simultaneously because the frozen solutions of the proteins correspond to a disordered state, implying a distribution of local environments for the active site and concomitant distributions of distances and angles defining its geometry. Then, inside this distribution of conformations, one part of them would favor one kind of localization and so on. This seems reasonable to use because we have seen in our irradiated crystals that, for the $[Fe_4S_4]^{3+}$ state, the differences in energy between the different trapping sites of the mixed-valence pair are apparently small.

This explanation differs very appreciably from the one given by Antanaïtis and Moss.[10a] In effect, these authors did not think that the two main signals 1 and 2 of the EPR spectra are associated with mixed-valence pairs having two different localizations. They considered, by contrast with our conclusions, that in the mixed-valence pair the valence state Fe(II) and the valence state Fe(III) are in the slow exchange regime, the unpaired electron shuttling back and forth with a characteristic time τ such that $10^{-7} > \tau \geq 10^{-8}$ s. Then, their interpretation was that the component 1 would be associated with a situation where the Fe(II) is placed on an individual site of predominately local axial symmetry, while the component 2 would be associated with a situation where it is on a site of locally distorted axial symmetry.

Supplementary elements coming from the last proton ENDOR studies made by some of us[5,8] on the irradiated crystals between 6 and 10 K must also be taken into account. In effect, one conclusion of these studies is that, within a simple description based on the symmetric vector model, the center IV and the center I must be ascribed to two different magnetic ground states, the first one being identified with the $|7/2, 3, 1/2\rangle$ magnetic state, while the second one would probably correspond to the $|9/2, 4, 1/2\rangle$ state.[24] This suggests that, in the *C. vinosum* and *C. tepidum* proteins, the axial signal 1 may correspond to the $|9/2, 4, 1/2\rangle$ state, while the rhombic and less anisotropic signal 2 may correspond to the $|7/2, 3, 1/2\rangle$ state. This conjecture is only based for the moment on analogies, and it certainly needs to be tested by new and supplementary measurements.

We want to add that there seems to exist a close relationship between the interpretation given there to the EPR spectrum of oxidized *C. vinosum* in low-temperature frozen solution and the one needed for its NMR spectrum at higher temperatures, i.e. in liquid solution around 300 K. Recently, Bertini et al. have been able to assign the β-CH_2 cysteine protons of this protein and to determine by this way which iron ions of the cluster are in the ferric state and which are those attributed to the mixed-valence pair.[25b,c] Thus, the mixed-valence pair appears to be localized on two particular iron atoms in the protein in solution, and the situation is, at first sight, reminiscent of the one found by EPR in our irradiated crystals; but, is the mixed-valence pair also completely localized and "frozen" on two particular irons in the proteins or is there some rapid dynamics (with respect to the NMR time scale) remaining under way but which would involve a predominant site of localization? This is a sound question because in liquid water around 300 K the protein backbone and the cysteine ligands undergo motions which are probably able to dynamically modulate the cubane geometry and to give rise to "jumps" of the mixed-valence pair between different sites of occupancy, like in the $[Fe_4S_4]^+$ synthetic models in which it is clear that these jumps occur.[26–28] This possibility of jumps of the mixed valence-pair has been evoked very recently by Bertini et al.[29] and Banci et al.[30] in order to explain—in oxidized *C. vinosum*[25] and in other high-potential proteins[29–31]—the striking difference in NMR shifts existing between one group of β-CH_2 cysteine protons bound to a ferric ion with respect to those bound to the second ferric ion. This hypothesis is an alternative proposal, of dynamical character, to the static model that they had considered previously, where this difference was rationalized with a Heisenberg Hamiltonian dissymmetrizing the roles of the two ferric ions.[31a] In their more recent proposal, there would be two positions of localization of the mixed-valence pair with fast exchange between them, the probabilities of occupancy of these two sites varying among the different proteins considered.[29,30] In principle, by analogy with the observations made by NMR in the synthetic model compounds, the six different sites of possible residence of the mixed-valence pair must be considered. But the peculiarity of the proteins is that the probabilities of occupancy of these six sites are probably quite different between them because the four cysteine ligands are constrained by the particular folding of the peptide skeleton and constitute an unsymmetrical environment for the cubane. This led us to consider that these jumps of the mixed-valence pair are possible and even likely in the proteins at room temperature. Thus, we also suggest that, in the NMR spectra of *C. vinosum* and *C. tepidum*, there is rapid

(23) We speculate that the third, small signal to which Antanaïtis and Moss attribute in their fits a nearly isotropic g-tensor with $g_{av} \approx 2.036$ may, in fact, be the $g_\perp^3$ value (or eventually the $g_\perp^4$ value) of an anisotropic signal.

(24) In this description, which corresponds to a simple and symmetrical vectorial spin coupling model involving two equivalent mixed-valence iron atoms and two equivalent ferric atoms, the first number represents the intermediate spin state of the mixed-valence pair and the second one the intermediate spin state of the ferric pair, while the last one corresponds to the resulting spin of the cluster.

(25) (a) Cowan, J. A.; Sola, M. *Biochemistry* **1990**, *29*, 5633. (b) Bertini, I.; Briganti, F.; Luchinat, C.; Scozzafava, A.; Sola, M. *J. Am. Chem. Soc.* **1991**, *113*, 1237. (c) Bertini, I.; Capozzi, F.; Ciurli, S.; Luchinat, C.; Messori, L.; Sola, M. *J. Am. Chem. Soc.* **1992**, *114*, 3332. (d) Nettesheim, D. G.; Harder, S. R.; Feinberg, B. A.; Otvos, J. D. *Biochemistry* **1992**, *31*, 1234.

(26) In all known NMR spectra of 4Fe–4S synthetic models in solution, each category of proton of a thiolate ligand is characterized by only one NMR line, whichever iron to which the thiolate ligand is bound. This is well illustrated for the $[Fe_4S_4]^+$ state in $[Et_4N]_3[Fe_4S_4(SCH_2C_6H_5)_4]$ (see ref 27) and also in other model compounds (see ref 28). In effect, we cannot distinguish in their spectra the proton NMR lines of the ligands bound to irons of the mixed-valence pair from those of the ligands bound to irons of the ferrous pair, which appear as all equivalent on the NMR time scale. Thus, in these solutions, the conformational movements of the ligands appear able to modulate sufficiently rapidly the cubane geometry so that the mixed-valence pair seems to "jump" between six positions which are equivalent. A similar situation is expected for NMR spectra of synthetic models in the $[Fe_4S_4]^{3+}$ state, but this cannot be ascertained since the NMR spectrum of the $[Fe_4S_4(S\text{-}2,4,6\text{-}(i\text{-}Pr)_3C_6H_2)_4]^-$ compound is not known.

(27) Reynolds, J. G.; Laskowski, E. J.; Holm, R. H. *J. Am. Chem. Soc.* **1978**, *100*, 5315.

(28) Hagen, K. S.; Watson, A. D.; Holm, R. H. *Inorg. Chem.* **1984**, *23*, 2984.

(29) Bertini, I.; Capozzi, F.; Luchinat, C.; Piccioli, M. *Eur. J. Biochem.* **1993**, *212*, 69.

(30) Banci, L.; Bertini, I.; Capozzi, F.; Carloni, P.; Ciurli, S.; Luchinat, C.; Piccioli, M. *J. Am. Chem. Soc.* **1993**, *115*, 3431.

(31) (a) Banci, L.; Bertini, I.; Briganti, F.; Luchinat, C.; Scozzafava, A.; Vicens Oliver M. *Inorg. Chem.* **1991**, *30*, 4517. (b) Bertini, I.; Capozzi, F.; Luchinat, C.; Piccioli, M.; Vicens Oliver, M. *Inorg. Chim. Acta* **1992**, *198–200*, 483.

exchange between different sites of localization of the mixed-valence pair which could be roughly the same as those characterized at low temperatures by EPR. However, we admit that, in first approximation, it is probably sufficient to consider only (like Banci et al.[30]) two components in order to attempt to interpret their NMR spectra, since the corresponding EPR spectra indicate that two components are greater than the others.

V-2. Comments on the EPR Spectra of the $[Fe_4S_4(S\text{-}2,4,6\text{-}(i\text{-}Pr)_3C_6H_2)_4]^-$ Synthetic Compound. We find it useful to discuss also, in the same spirit as above, the EPR spectra of the $[Fe_4S_4]^{3+}$ state in the $[Fe_4S_4(S\text{-}2,4,6\text{-}(i\text{-}Pr)_3C_6H_2)_4]^-$ model compound studied by Papaefthymiou et al.[15] These spectra are also rather strange because they show a striking and unusual variability between the two different physical conditions under which they are examined. In effect, if we consider the spectrum of the compound in frozen toluene solution, it has been fitted with $g_1 = 2.10$, $g_2 = 2.05$, and $g_3 = 2.03$. It is completely different from the polycrystalline spectrum, which has been fitted with $g_1 = 2.065$, $g_2 = 1.97$, and $g_3 = 1.96$. Thus, two different experimental conditions give rise to two very different $[Fe_4S_4]^{3+}$ species. We can remark that the polycrystalline sample has a g_1 value very similar to the one of center IV, while its g_2 and g_3 values are much lower than those of this center and are rather unusual for $[Fe_4S_4]^{3+}$ states. By contrast, the g-values corresponding to the frozen toluene solution are reminiscent of the values of the center III. Moreover, in spite of the broadness of the frozen solution spectrum, its careful inspection (see ref 15) shows that one additional shoulder feature is present at low field, indicating that this spectrum contains more than one component. The differences observed between the frozen solution and the polycrystalline spectra must be ascribed to differences in the geometry of the cubane and in the conformations of its ligands, crystal packing effects certainly influencing the polycrystalline spectrum. They indicate once more the sensitivity of the $[Fe_4S_4]^{3+}$ state to geometrical and conformational variations which appears sufficient to give rise to quite different g-tensors.

VI. Conclusion

Two families of paramagnetic centers corresponding respectively to the $[Fe_4S_4]^{3+}$ and $[Fe_4S_4]^{+}$ oxidation states have been detected and studied in γ-irradiated single crystals of the $[(C_2H_5)_4N]_2[Fe_4S_4(SCH_2C_6H_5)_4]$ compound and its partially and fully deuterated counterparts. We have characterized up to five or six different $[Fe_4S_4]^{3+}$ paramagnetic species which correspond to the oxidized state of the high-potential proteins. Moreover, two different $[Fe_4S_4]^{+}$ species are also observed which correspond to the reduced state of the ferredoxins.

It is noteworthy to observe that no free radical is formed at the level of either the thiolate ligands or the counterions, even at very high doses of irradiation. This indicates that the energy of the γ rays is used to produce ionization processes which operate exclusively at the level of the cubane clusters and which do not lead to heterolytic bond scissions giving rise to radicals in the organic parts. Thus, the iron–sulfur cubanes apparently protect completely their environment from radiation damage. Obviously, this observation must be put together with their most remarkable property, i.e. their facility to lose or gain one electron that nature uses so remarkably in the proteins.

The g-tensors of the different $[Fe_4S_4]^{3+}$ and $[Fe_4S_4]^{+}$ centers present a common feature: the principal direction $\vec{V}_1$ associated with their greatest principal value g_1 is near the direction of an idealized C_2 axis of symmetry perpendicular to the direction of the mixed-valence pair of iron atoms and to the direction of the ferric pair. Their multiplicity corresponds to different possibilities of trapping the mixed-valence pair $Fe^{2.5+}$–$Fe^{2.5+}$ on two particular iron atoms of the cluster. The results obtained on the $[Fe_4S_4]^{3+}$ centers have also led us to propose a new interpretation of the composite EPR spectra of the oxidized high-potential *C. vinosum* and *C. tepidum* proteins due to four different localizations of the mixed-valence pair on the irons of the active site.

Concerning the $[Fe_4S_4]^{+}$ centers, the most striking fact (already found for the center A in the irradiated crystals of the $(Bu_4N)_2[Fe_4S_4(SC_6H_5)_4]$ compound[1,2]) is that these two centers are in the pure $S_{total} = 1/2$ state. They differ from a majority of synthetic compounds prepared in the $[Fe_4S_4(SR)_4]^{3-}$ state which show pure $S_{total} = 3/2$ states or "spin-admixed" states,[32] and from proteins like the Fe nitrogenase from *Azotobacter*, which shows the 1/2 and 3/2 states,[33] and the reduced selenium-reconstituted ferredoxin from *Clostridium pasteurianum*, which shows the 1/2, 3/2, and 7/2 states.[34] Carney et al.[32] have tried to find empirical correlations between the geometry of several $[Fe_4S_4(SR)_4]^{3-}$ complexes and their spin states. Our present observations of pure $S = 1/2$ states in a compound containing $[Fe_4S_4]^{2+}$ cubanes of idealized tetragonal symmetry[12] are in good agreement with their observations. But they have also tried to relate the spin state to the dihedral angles β = S*–Fe–S–C defining the ligand conformations. They have reported that β values in the 160–180° range would be associated with states with $S_{total} = 3/2$ and with "spin-admixed" states.[32] For the centers I_R and II_R corresponding to $S_{total} = 1/2$ states, the S–C bonds are also in the staggered configuration in the crystal structure with respect to the Fe–S* ones (β = 177, 173, 177, and 171°).[35] Thus, these results suggest that the dihedral angles β might not be significant parameters.

Following a suggestion made by a reviewer, which we acknowledge, let us add that the detection of the two different centers I_R and II_R can also shed some light on the existence of a minority species characterized by a $g_1 = 2.04$ which was detected in addition to the main species in the $[Fe_4S_4]^{+}$ state of *Desulfovibrio gigas* ferredoxin I.[36] This minority signal would correspond to a second possibility of localization of the mixed-valence pair with respect to the one associated with the main species.

Acknowledgment. We are indebted to Gérard Desfonds and to Gérard L'Hospice for their contributions to the material realization of this work. We thank Jean Laugier and Joël Moulin for their determination of the crystal morphology. We want to thank our collegues, Jacques Gaillard, Jacques Meyer, Jean-Marc Moulis, and also Louis Noodleman from the Research Institute of Scripps Clinic (La Jolla, CA) for numerous and interesting discussions on various parts of this work. We want to thank the NATO organization for the obtention of a Collaborative Research Grant (CRG 910204) with the Research Institute of Scripps Clinic on this subject.

(32) (a) Carney, M. J.; Papaefthymiou, G. C.; Spartalian, K.; Frankel, R. B.; Holm, R. H. *J. Am. Chem. Soc.* **1988**, *110*, 6084. (b) Carney, M. J.; Papaefthymiou, G. C.; Frankel, R. B.; Holm, R. H. *Inorg. Chem.* **1989**, *28*, 1497.

(33) (a) Lindahl, P. A.; Day, E. P.; Kent, T. A.; Orme-Johnson, W. H.; Münck, E. *J. Biol. Chem.* **1985**, *260*, 11160. (b) Meyer, J.; Gaillard, J.; Moulis, J.-M. *Biochemistry* **1988**, *27*, 6150. (c) Lindahl, P. A.; Gorelick, N. J.; Münck, E.; Orme-Johnson, W. H. *J. Biol. Chem.* **1987**, *262*, 14945.

(34) Meyer, J.; Moulis, J.-M.; Gaillard, J.; Lutz, M. *Adv. Inorg. Chem.* **1992**, *38*, 74 and references cited therein.

(35) This comparison supposes that the structures of the paramagnetic centers only differ by minor changes with respect to the one given by the crystallographic study. This hypothesis has been verified for the center IV by its detailed proton ENDOR study (see ref 5).

(36) Moura, J. J. G.; Moura, I.; Kent, T. A.; Lipscomb, J. D.; Huynh, B. H.; LeGall, J.; Xavier, A. V.; Münck, E. *J. Biol. Chem.* **1982**, *257*, 6259.